DOI: 10.1002/ejic.200500671

Solid-State Luminescence and π-Stacking in Crystalline Uranyl Dipicolinates

Jack M. Harrowfield,*[a] Noël Lugan,[b] Gholam H. Shahverdizadeh,[c] Ali A. Soudi,[c] and Pierre Thuéry[d]

Keywords: Uranyl luminescence / Crystal structures / π-Stacking / Dipicolinates

Crystal structure determinations on the hydrated forms of the complexes $M_2UO_2(dipic)_2$, M = H, Rb, Cs, dipic = dipicolinate = pyridine-2,6-dicarboxylate, all of which show strong solid-state luminescence from the uranyl centre, have as a common feature extended π-stacking arrays of the dipicolinate ligands. Comparisons with related but non-luminescent complexes indicate that these stacking arrays may be associated with efficient energy transfer from the dipicolinate "antennae" to the uranyl unit.

Introduction

Pyridine-2,6-dicarboxylic acid (dipicolinic acid, $dipicH_2$) is a widely employed and versatile complexing agent known to bind in its singly, doubly and even non-deprotonated and diester forms, often as mixed-ligand species.[1–5] Related ligands such as chelidamic acid (4-hydroxypyridine-2,6-dicarboxylic acid) and benzimidazole derivatives of dipicolinate also display interesting coordination properties.[6,7] Dipicolinic acid and its anions appear to bind well to all metals in the periodic table, though specific properties such as the strong luminescence of Eu^{III} and Tb^{III}[8] and the biological activity of transition-metal complexes[3,9,10] have led to a strong focus in certain areas and to a relative neglect of actinide complexation. Nonetheless, in the specific case of the uranyl ion, a variety of species,[11–14] including the remarkable helical polymer, $[UO_2(dipic)(OH_2)]_n$,[15] has long been known and has recently been significantly expanded, principally through the characterisation of several binuclear complexes.[16] During a structural study, reported herein, of further members of the dipicolinate family, we noted that one property of these compounds that varies strikingly is their solid-state luminescence and hence we have attempted to rationalise this through an analysis of the different lattices.

Results and Discussion

A particularly useful technique for the production of crystals of rather insoluble metal complexes has proven to be the "branched tube" method[17] of diffusion along a thermal gradient.[18] In the extension of this procedure used here to uranyl complexes of dipicolinic acid, the product obtained from a mixture of reagents with a 1:2 ratio of U^{VI}/acid was found to be a mixture of crystalline materials, one of which was a complex containing the metal and ligand in this ratio but the other a 1:1 species. Both can also be obtained by direct reaction of $[UO_2(OH_2)_5]^{2+}$ with the appropriate ligand species in these different ratios in aqueous solution; the 1:2 complex appears to be of very low solubility and crystallising readily, whereas the 1:1 complex appears to be more soluble and deposits rather slowly. Structure determinations (Table 1) on crystals selected from the mixed product showed the 1:1 species, which crystallises as clusters of very fine, pale yellow needles, to be the known helical polymer, $[UO_2(dipic)(OH_2)]_n$,[15] and the 1:2 species, which crystallises as obviously greenish-yellow plates, to be $[UO_2(dipicH)_2]·4H_2O$. The dipicolinate units function as tridentate ligands in both cases, the uranium coordination environment being close to pentagonal bipyramidal UNO_6 in the 1:1 complex and close to hexagonal bipyramidal UN_2O_6 in the 1:2 complex.

The lattice of $[UO_2(dipicH)_2]·4H_2O$ is similar to that of $[NH(C_2H_5)_3]_2[UO_2(dipic)_2]·2H_2O$[16] (both crystals being monoclinic, space group *C*2/*c*, though they are not isomorphous) as is emphasised by a view down *c* (Figure 1). Hydrogen bonding in the lattice of the latter compound has been analysed in detail and the protons of the triethylammonium groups appear to form near-symmetrical bridges between the coordinated oxygen atoms of opposite dipicolinate units within the one complex unit. The complex can thus be considered to have a "pseudo-macrocyclic" form

---

[a] Laboratoire de Chimie Supramoléculaire, UMR 7006 du CNRS, Institut de Science et d' Ingénierie Supramoléculaires,
8 allée Gaspard Monge, 67083 Strasbourg, France
[b] Laboratoire de Chimie de Coordination du CNRS, UPR 8241 du CNRS,
205 route de Narbonne, 31077 Toulouse Cedex 04, France
[c] Department of Chemistry, University of Zanjan,
P. O. Box 49195, Zanjan, Iran
[d] CEA/Saclay, DSM/DRECAM/SCM, URA 331 du CNRS, Bât. 125,
91191 Gif-sur-Yvette, France

Supporting information for this article is available on the WWW under http://www.eurjic.org or from the author.

Table 1. Crystal data and structure refinement details.

Empirical formula	$C_{14}H_{16}N_2O_{14}U$	$C_7H_5NO_7U$	$C_{14}H_{12}N_2O_{13}Rb_2U$	$C_{14}H_{14}Cs_2N_2O_{14}U$
Formula weight	674.32	453.15	825.23	938.12
T [K]	180(2)	180(2)	100(2)	100(2)
Crystal system	monoclinic	hexagonal	monoclinic	triclinic
Space group	$C2/c$	$P6_1$	$C2/c$	$P\bar{1}$
a [Å]	18.5189(9)	14.7245(7)	19.1824(8)	6.7725(3)
b [Å]	6.8384(3)	14.7245(10)	14.7980(6)	8.4145(5)
c [Å]	15.4943(9)	9.2583(9)	7.5167(2)	10.8428(7)
α [°]	90	90	90	99.127(3)
β [°]	94.353(4)	90	111.114(3)	106.607(4)
γ [°]	90	120	90	110.102(3)
V [Å^3]	1956.53(17)	1738.4(2)	1990.45(13)	532.93(6)
Z	4	6	4	1
$D_{calcd.}$ [Mg·m^{-3}]	2.289	2.597	2.754	2.923
μ(Mo-$K\alpha$) [mm^{-1}]	8.375	14.024	13.089	11.057
F(000)	1272	1212	1520	426
Crystal size [mm^3]	$0.26 \times 0.24 \times 0.10$	$0.64 \times 0.09 \times 0.07$	$0.17 \times 0.11 \times 0.09$	$0.15 \times 0.12 \times 0.06$
θ Range for data collection	3.18–32.09	3.20–32.00	3.04–25.68	3.39–25.68
Index ranges	$-26 \le h \le 27$ $-10 \le k \le 10$ $-22 \le l \le 18$	$-21 \le h \le 21$ $-21 \le k \le 19$ $-13 \le l \le 13$	$0 \le h \le 23$ $0 \le k \le 18$ $-9 \le l \le 8$	$0 \le h \le 8$ $-10 \le k \le 9$ $-13 \le l \le 12$
Reflections collected	19458	18751	22423	16850
Independent reflections	3188	3833	1884	2020
R_{int}	0.039	0.092	0.034	0.049
Completeness to θ_{max} (%)	92.9	97.6	99.8	99.8
Absorption correction	analytical	semi-empirical	empirical	empirical
$T_{max.}/T_{min.}$	0.462/0.118	0.349/0.090	0.308/0.086	0.515/0.106
Restraints/parameters	0/142	1/145	0/147	0/151
Goodness-of-fit on F^2	1.043	1.086	1.287	1.294
R_1/wR_2 [$I > 2\sigma(I)$]	0.023/0.054	0.039/0.089	0.026/0.103	0.028/0.121
R_1/wR_2 (all data)	0.025/0.055	0.045/0.092	0.028/0.104	0.028/0.121
$\Delta\rho_{max.}/\Delta\rho_{min.}$ [e·Å^{-3}]	0.98/–2.23	2.10/–1.68	0.93/–1.30	1.12/–0.88
Flack parameter		0.01(2)		

somewhat like that well-known in M^{II} complexes of the dimethylglyoxime monoanion.[19] In [UO_2(dipicH)$_2$]·$4H_2O$, while a water molecule bridges the coordinated oxygen atoms to give a similar form (Figure 2), in addition the residual acid protons appear to be located on the outer (uncoordinated) carboxylate oxygen atoms, O(3), and to be involved in H-bonding chains involving two water molecules and the confronting O(3′) atoms, defining another mode of formation of a "pseudo-macrocycle". The potentially more rigid resulting structure is associated with a closer approach to planarity of the U(dipicH)$_2$ unit, although it is both slightly bowed [N–U–N 174.05(8)°] and twisted into a chiral configuration, as is the case for the U(dipic)$_2$ unit in [$NH(C_2H_5)_3$]$_2$[UO_2(dipic)$_2$]·$2H_2O$, but there the bowing is more marked [N–U–N 165.21(10)°]. The H-bonded water molecule pairs which bridge complex ion units intramolecularly are also within H-bonding distances of carboxylate oxygen atoms of other complex units, so linking the lattice in at least two dimensions.

Perhaps significantly, H-bonding is not the only form of extended interaction apparent in the lattice. Parallel to c, the complex units can be considered to form undulating columns [for example, within the ovoid entities apparent in the view down c (Figure 1)] in which there is considerable overlap of parallel dipicolinate rings of adjacent complexes of alternating chirality. This stacking[20,21] extends down b, so that there are two types of ring projections (Figure 3), describable as intra- and inter-ovoid, contributing to the formally infinite array. While projection of one ring onto its parallel neighbour in a given stack does not involve eclipsing of all atoms, there are numerous C···C contacts of <3.5 Å, associated in the case of the more strongly overlapped intra-ovoid array with an inter-centroid distance of 3.63 Å and a centroid offset of 1.35 Å. It is especially in this regard that the lattice differs from the remarkably beautiful lattice of [UO_2(dipic)(OH_2)]$_n$.[15] In the present redetermination of this structure, the crystal chosen was one in which the helical polymer units (Figure 4) present were all right-handed, with the pitch of the helices [9.26(1) Å] being such that projecting dipicolinate units are very remote. These helices interlock to some extent in a way which involves no short contacts between constituent atoms of the dipicolinate rings (shortest inter-centroid distance 5.54 Å), though there are some involving C and O of the carboxylate units. Instead, there is a rather short contact [3.04(1) Å] of one uranyl-*O* to ring atom C2 [as well as UO···N of 3.09(1) Å]. Such uranyl group interactions are seen in other systems[22] and indeed in [UO_2(dipicH)$_2$]·$4H_2O$, there are longer UO···C(aromatic) approaches of 3.17(1) Å, though essentially in the plane of the ring.

Such points of difference between [UO_2(dipicH)$_2$]·$4H_2O$ and [UO_2(dipic)(OH_2)]$_n$ may be the cause of their marked difference in solid-state luminescence. Thus, 354 nm (Hg lamp) irradiation of [UO_2(dipicH)$_2$]·$4H_2O$ produces bright green luminescence characteristic of a uranyl centre[23] (and the greenish colour of the crystals under solar illumination

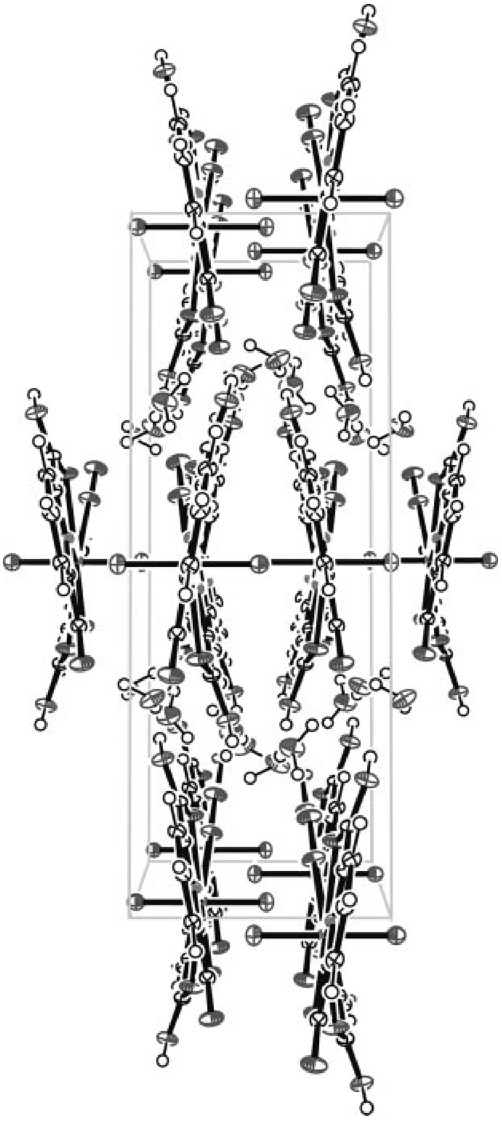

Figure 1. A view, down *c*, of the lattice of $[UO_2(dipicH)_2]{\cdot}4H_2O$ which displays the columnar structures of ovoid cross-section present. Displacement ellipsoids are drawn at the 50% probability level. H atoms are shown with arbitrary radii of 0.1 Å.

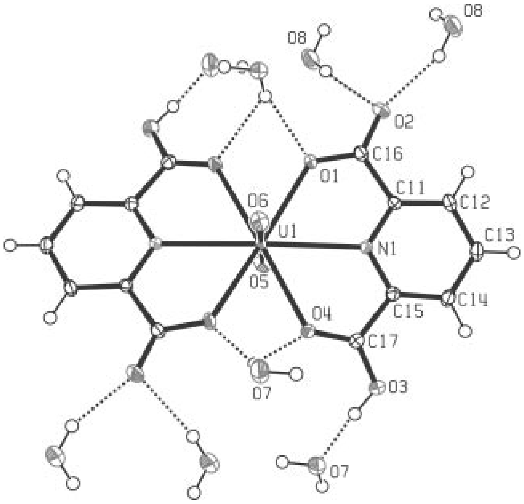

Figure 2. The hydrogen-bonding array present in the lattice of $[UO_2(dipicH)_2]{\cdot}4H_2O$ (displacement ellipsoids at the 50% probability level).

may be explained as of the same origin), with the principal emission maxima at 487, 509, 532 and 558 nm (Figure 5) being a much closer match to those of hexagonal bipyramidal U^{VI} as in $[UO_2(NO_3)_2(OH_2)_2]$[24] than to those of pentagonal bipyramidal U^{VI} as in $[UO_2(OH_2)_5]^{2+}$[23]. $[UO_2(dipic)(OH_2)]_n$ is not luminescent by eye under the same conditions, though very weak luminescence, with maxima at 465, 490, 515 and 535 nm can be detected by use of a fluorimeter. Obviously, issues such as the presence of two dipicolinate ligands in the first and of a possibly electronically deactivating aqua ligand in the second (though even in the case of $[UO_2(OH_2)_5]^{2+}$, [23b] this does not seem to apply) must be considered, and then it is important to note that neither complex is strongly luminescent in aqueous solution. Further, deprotonation of $[UO_2(dipicH)_2]$ with $[NBu_4][OH]$ to produce a chloroform-soluble species, for which the electrospray mass spectrum (Supporting Information; for Supp. Inf. see also the footnote on the first page of this article) in this solvent shows a parent peak of the dianion, also results in loss of emission (thus excluding the possibility that the negligible luminescence in water is a consequence of deactivation by bound water after ligand hydrolysis), though evaporation of this solution produces a luminescent solid. Thus, even if dipicolinate units as "antennae" for energy absorption and transfer to the uranyl emissive state are only efficient when there are at least two per uranium atom, this efficiency must be associated with the solid-state structure. This is true also for $[NH(C_2H_5)_3]_2[UO_2(dipic)_2]{\cdot}2H_2O$, which is luminescent as the solid,[25] again differing in this regard from several binuclear species having a single dipicolinate ligand per uranium.[16] In the lattices of these binuclear species, it is possible to discern parallel arrays of dipicolinate entities indicative of stacking interactions but, significantly, these all involve either relatively remote atom···atom contacts (>3.5 Å) or limited overlaps or pairwise interactions in one-dimensional arrays, unlike the extended two-dimensional arrays described above for $[UO_2(dipicH)_2]{\cdot}4H_2O$ and which can also be discerned in $[NH(C_2H_5)_3]_2[UO_2(dipic)_2]{\cdot}2H_2O$. [In the first complex, there are also O(carboxylate)···C(aromatic) contacts ca. 3.3 Å which produce a third dimension to the interactions between the aromatic entities.] In all the complexes presently discussed, there are UO···C(aromatic) contacts between 3.0 and 3.4 Å which vary in a way which seems unrelated to the luminescence properties of the solids. Thus, it would seem plausible that strong uranyl emission in these complexes is an indicator of extended stacking interactions with significant electronic consequences

An indication of the utility of the branched-tube method for crystal formation was provided in efforts to extend characterisation of the $M_2UO_2(dipic)_2$ family to the cases where M is an alkali metal cation. All (M = Li, Na, K, Rb, Cs) these compounds are of low water solubility and precipitate very rapidly as green, luminescent materials, of very similar

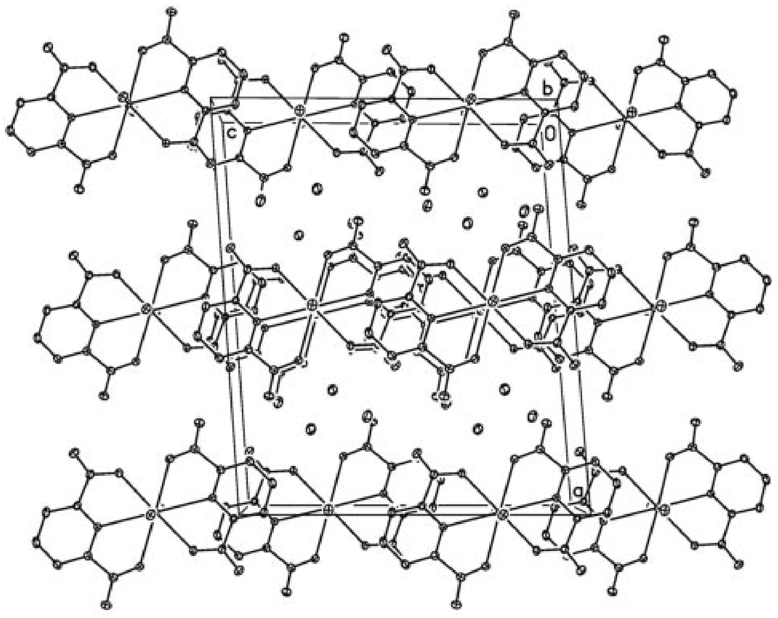

Figure 3. A view, perpendicular to the mean ring planes, showing the two types of dipicolinate stacks ("intra-" and "inter-ovoid") in the lattice of $[UO_2(dipicH)_2]\cdot 4H_2O$. The greater degree of ring overlap corresponds to the intra-ovoid stacks (displacement ellipsoids at the 50% probability level).

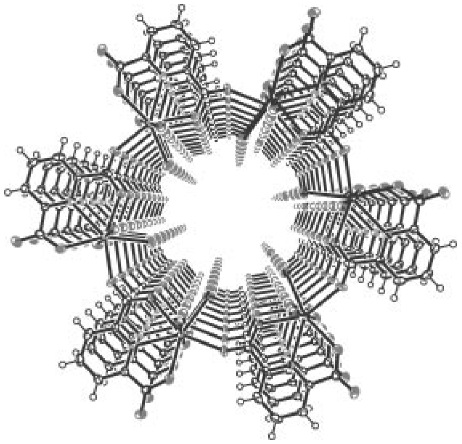

Figure 4. A view down the axis of one of the (right-handed) infinite helices present in the lattice of $[UO_2(dipic)(OH_2)]_n$ (displacement ellipsoids at the 50% probability level).

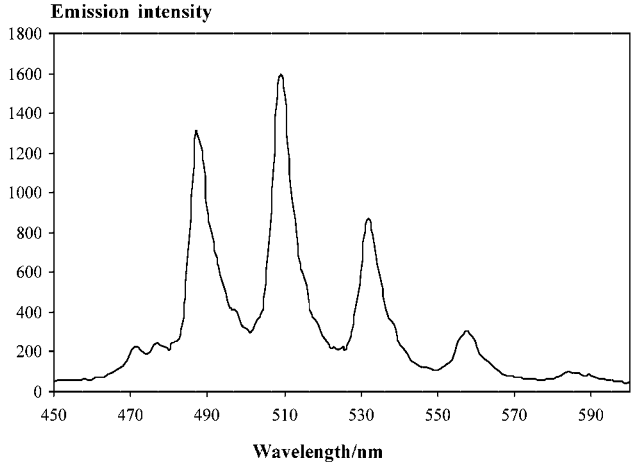

Figure 5. The room-temperature luminescence spectrum of powdered $[UO_2(dipicH)_2]\cdot 4H_2O$. Excitation wavelength 320 nm.

appearance to the M = H complex, when hot solutions are cooled. Despite numerous attempts at careful recrystallisation, the only members of this series obtained in a form suitable for X-ray structure determinations in this way were the Rb and Cs species (Table 1). While the Rb complex retains the same space group ($C2/c$) as the triethylammonium and proton compounds, the Cs complex crystallises in $P\bar{1}$, though this has only rather minor consequences in terms of the structure and self-interactions of the $U(dipic)_2$ entities. In both the Rb and Cs complexes, the $U(dipic)_2$ units are planar, with N–U–N 180° due to the location of the uranium atom on a symmetry centre. Perhaps as a reflection of this move to coplanarity, the U–N bond lengths (Table 2) are the longest of any in a uranyl dipicolinate. Their extension, however, is slight, and U–O bond lengths (Table 2) fall essentially within the range of those in other $U(dipic)_2$ species.

However, the Rb and Cs complexes do differ most obviously in the orientation of chains of the alkali metal atoms with respect to the array of $[UO_2(dipic)_2]^{2-}$ units. (Figure 6). Viewed down *c*, for example, both lattices can be regarded as containing sheets of uranium atoms lying parallel to [100], each U atom visible in the view down *c* being the head of a column of such atoms lying parallel to *c*. Using the two shortest (and nearly equal) M···M separations [M = Rb, 4.0926(12) and 4.4260(12); M = Cs, 4.3109(9) and 4.9406(9) Å] to define association between M atoms, these can be considered to form zig-zag columns which, in the

Table 2. Selected bond lengths [Å] and angles [°].

$[UO_2(dipicH)_2]\cdot 4H_2O$[a]	U(1)–O(1)	2.441(2)	O(1)–U(1)–N(1)	60.77(7)
	U(1)–O(4)	2.499(2)	N(1)–U(1)–O(4)	60.42(7)
	U(1)–O(5)	1.769(3)	O(1)–U(1)–O(4′)	60.45(7)
	U(1)–O(6)	1.782(3)	O(5)–U(1)–O(6)	180
	U(1)–N(1)	2.641(2)		
$[UO_2(dipic)(OH_2)]$[b]	U(1)–O(1)	2.380(6)	O(1)–U(1)–N(1)	63.30(19)
	U(1)–O(4)	2.416(5)	N(1)–U(1)–O(4)	63.66(19)
	U(1)–O(5)	1.775(6)	O(4)–U(1)–O(7)	73.9(2)
	U(1)–O(6)	1.768(6)	O(7)–U(1)–O(3′)	77.5(2)
	U(1)–O(7)	2.423(6)	O(3′)–U(1)–O(1)	81.9(2)
	U(1)–N(1)	2.520(6)	O(5)–U(1)–O(6)	178.4(3)
	U(1)–O(3′)	2.340(6)		
$[UO_2Rb_2(dipic)_2(H_2O)_3]$[c]	U–O(1)	2.445(5)	O(1)–U–N(1)	59.64(14)
	U–O(3)	2.466(5)	N(1)–U–O(3)	59.65(16)
	U–O(5)	1.783(6)	O(1)–U–O(3′)	60.72(15)
	U–N(1)	2.657(5)	O(5)–U–O(5′)	180
	Rb–O(1)	3.129(5)	Rb–O(5)	3.035(6)
	Rb–O(2′′)	3.046(4)	Rb–O(6)	2.849(5)
	Rb–O(3′)	3.006(5)	Rb–O(6$^{\$}$)	2.914(5)
	Rb–O(4$^{\#}$)	2.927(5)	Rb–O(7)	2.813(5)
$[UO_2Cs_2(dipic)_2(H_2O)_4]$[d]	U–O(1)	2.435(5)	O(1)–U–N(1)	59.67(16)
	U–O(3)	2.466(5)	N(1)–U–O(3)	60.01(16)
	U–O(5)	1.765(5)	O(1)–U–O(3′)	60.33(15)
	U–N(1)	2.669(6)	O(5)–U–O(5′)	180
	Cs–O(1)	3.143(5)	Cs–O(6)	3.211(5)
	Cs–O(2)	3.439(5)	Cs–O(6$^{\$}$)	3.390(5)
	Cs–O(2′′)	3.115(5)	Cs–O(6′′)	3.426(6)
	Cs–O(3′)	3.207(5)	Cs–O(7)	3.037(5)
	Cs–O(4$^{\#}$)	3.307(5)	Cs–O(7*)	3.399(6)
	Cs–O(4′)	3.717(5)		

[a] Symmetry code: ′ for –*x* – 1, *y*, –*z* – 1/2. [b] Symmetry code: ′ for *y* + 1, –*x* + *y* + 1, *z* – 1/6. [c] Symmetry codes: ′ for 1/2 – *x*, 3/2 – *y*, –*z*; ′′ for *x*, 1 – *y*, *z* + 1/2; $^{\#}$ for *x* – 1/2, 3/2 – *y*, *z* – 1/2; $^{\$}$ for –*x*, *y*, 1/2 – *z*. [d] Symmetry codes: ′ for 1 – *x*, –*y*, –*z*; ′′ for 2 – *x*, 1 – *y*, 1 – z; $^{\#}$ for 1 + *x*, *y*, 1 + *z*; $^{\$}$ for 3 – *x*, 1 – *y*, 1 – *z*; * for 2 – *x*, –*y*, 1 – *z*.

case of M = Rb, lie along *c* and so define sheets for which the mean plane is parallel to those of the U atoms, i.e. to [100], whereas in the case of M = Cs these zig-zag columns lie parallel to *b*, forming undulating sheets with their mean planes parallel to [001]. An explanation of the difference in these alkali metal arrays may be that only Rb is involved in coordinative interaction with uranyl-*O* [Rb–O 3.035(6) Å]. As seems to be commonly the case with heavy and apparently weakly coordinating metals, [6,21,27–31] it is difficult to define a precise cutoff distance for interactions considered to be bonding but the coordination numbers of both Rb and Cs here appear to be high, involving *O*-donors only, with rather irregular geometry about the metals. Interestingly, the extreme M···O separations approach those of M···U, which, if they are correctly considered as contacts of closed-shell species of similar charge, would be regarded as involving negligible interactions, thus indicating that the extreme M···O contacts must also be of little significance.

In relation to development of the argument presently that uranyl luminescence in solid dipicolinate complexes may be associated with extended interactions of the dipicolinate "antennae", it is important to note that both the Rb and Cs complexes share with other luminescent uranyl dipicolinate species an essentially infinite stacked array of dipicolinates involving numerous relatively short C···C approaches (ca. 3.4 Å), corresponding in both compounds to a shortest centroid···centroid distance of 3.76 Å and centroid offsets of 1.37 and 1.62 Å for the Rb and Cs complexes, respectively. In the Rb complex, this stacking is apparent in the view down *c*, this axis being close to perpendicular to the mean ring planes, whereas in the Cs complex, it is a view down *a*, which exposes a similar array.

Conclusions

If indeed it is true that stacking within the lattices of uranyl dipicolinates can produce efficient population of uranyl excited states, then these generally rather insoluble materials may have applications as solid photocatalysts, as recently described for some mixed U/Ag compounds also characterised by extended ligand stacking within the crystals.[26] Even more recently,[32] some uranyl complexes of isomeric (2,4- and 3,4-)pyridine dicarboxylates, though of different stoichiometry to the present materials, have also been described as luminescent due to uranyl centre emission. Though stacking of the pyridine units is extended in these solids, the ring atom separations are relatively large (ca. 3.7 Å) and the compounds are described as yellow, indicating that their luminescence is weak and that their polyuranate cores may not be as effective as $[UO_2(dipic)_2]^{2-}$ in creating lattices which may be considered to contain "antenna" units of the ligands. The stoichiometry of bis(dipicolinato)dioxouranium(VI) derivatives is obviously open to straightforward variations which may result in useful control of their photoreactivity and we are presently investiga-

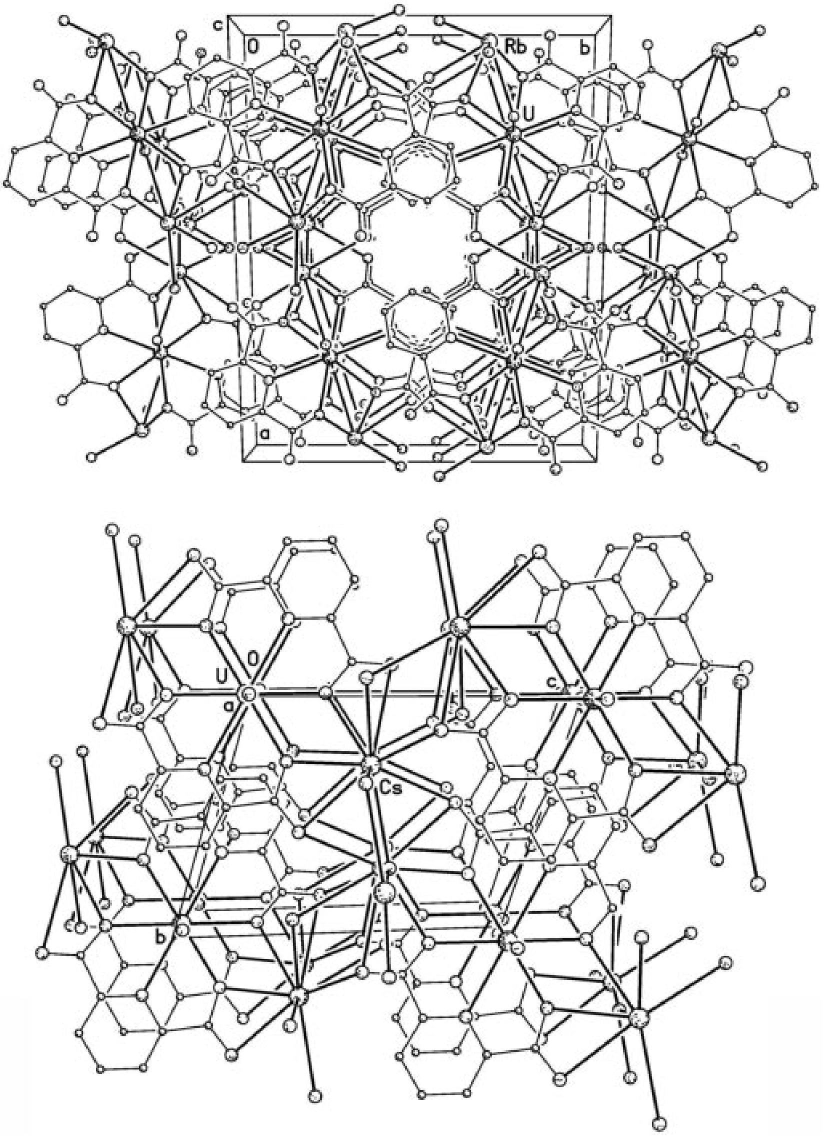

Figure 6. (top) The lattice of [$UO_2Rb_2(dipic)_2(H_2O)_3$], viewed down *c*. (bottom) The lattice of [$UO_2Cs_2(dipic)_2(H_2O)_4$], viewed down *a* (displacement ellipsoids at the 50% probability level).

ting lanthanide(III) species in which it appears possible to switch between uranyl and lanthanide ion luminescence.

Experimental Section

Synthesis: [$UO_2(dipicH)_2$]·$4H_2O$ and [$UO_2(dipic)(OH_2)$] (mixed): [$UO_2(O_2CCH_3)_2(OH_2)$]·H_2O (212 mg) and dipicolinic acid (167 mg) were placed in one arm of an inverted Y-tube ("branched tube"[17]) and the apparatus then carefully filled with water. The arm containing the partially soluble reactants was heated at 45 °C, with the other arm kept at ambient temperature. After 1 week, the cooler arm contained greenish-yellow plates mixed with clusters of pale yellow needles. Samples of both crystals were withdrawn for structure determinations, these showing the plates to be the new complex [$UO_2(dipicH)_2$]·$4H_2O$.

[$UO_2(dipicH)_2$]·$4H_2O$: A solution obtained by mixing dipicolinic acid (34 mg) and Na_2CO_3 (11 mg) in water (2 mL) and heating to 90 °C was mixed with a solution of [$UO_2(dmso)_5$](ClO_4)$_2$[22] (86 mg) in water (2 mL, 90 °C). The clear, pale yellow solution was allowed to stand at ambient temperature as plate-like crystals slowly deposited in essentially quantitative yield. After air-drying only, analysis of the sample was consistent with a higher degree of hydration than that of the single crystal taken for the structure determination. [$UO_2(dipicH)_2$]·$7H_2O$: calcd. C 23.09, H 3.04, N 3.85; found: C 22.9, H 2.8, N 3.5.

$M_2UO_2(dipic)_2\cdot nH_2O$ (M = Li, Na, K, Rb, Cs): Clear solutions, obtained by mixing dipicolinic acid ($2\cdot10^{-4}$ mol) and M_2CO_3 ($2\cdot10^{-4}$ mol) in water (2 mL) and heating at 90 °C until CO_2 evolution was complete, were mixed separately with solutions of [$UO_2(dmso)_2(NO_3)_2$] (10^{-4} mol; 55 mg) in hot (90 °C) water (2 mL). Cooling of the mixtures led to rapid and essentially quantitative precipitation of microcrystalline greenish-yellow solids. Partial precipitation resulting when the initial solutions were allowed to slowly evaporate at 90 °C provided larger but still generally rather small crystals. On collection and washing with acetone, the crystals appeared to undergo some efflorescence, and analyses of the Rb and Cs compounds indicated a lower degree of hydration than found from the structure solutions. $Li_2UO_2(dipic)_2$·$2H_2O$: calcd. C 25.86 (26.0); H 1.55 (2.0); N 4.31 (4.3); found C 26.0, H 2.0, N 4.3. $Na_2UO_2(dipic)_2$: calcd. C 26.02, H 0.94, N 4.33; found C 25.9, H 1.8, N 4.3. $K_2UO_2(dipic)_2$·$1.5H_2O$: calcd. C 23.84, H 1.28, N 3.97; found C 23.9, H 2.0, N 3.9. $Rb_2UO_2(dipic)_2$: calcd. C 21.80, H 0.85, N 3.63; found C 21.8, H 1.3, N 3.5. $Cs_2UO_2(dipic)_2$·H_2O: calcd. C 19.02, H 0.91, N 3.17; found C 19.4, H 1.3, N 2.9.

Luminescence Measurements: To obtain luminescence spectra for solid samples, the powdered complexes were pressed between two quartz plates with a spacing of ca. 0.1 mm. The plates were mounted in the normal cell holder of an AMINCO-Bowman Series 2 fluorimeter with the faces at 45° to the incident beam.

Crystallography: Intensities for both $[UO_2(dipicH)_2]$·$4H_2O$ and $[UO_2(dipic)(OH_2)]$ were collected at 180(2) K with an Oxford Diffraction Xcalibur diffractometer using graphite-monochromated Mo-K_α radiation (λ = 0.71073 Å). Cell refinement and data processing were performed using Crysalis RED.[33] All subsequent calculations were carried out using the WinGX system.[34] The structures were solved by using the SIR92 program,[35] which revealed in each instance the position of most of the non-hydrogen atoms. All remaining non-hydrogen atoms were located by the usual combination of full-matrix least-squares refinement and difference electron density syntheses by using the SHELXL97 program.[36] Atomic scattering factors were taken from the usual tabulations. Anomalous dispersion terms for U atoms were included in F_c. Analytical[37] ($[UO_2(dipicH)_2]$·$4H_2O$) or semi-empirical[38] ($[UO_2(dipic)(OH_2)]$) absorption corrections were applied.

The data for $[UO_2Rb_2(dipic)_2(H_2O)_3]$ and $[UO_2Cs_2(dipic)_2(H_2O)_4]$ were collected at 100(2) K with a Nonius Kappa-CCD area detector diffractometer[39] using graphite-monochromated Mo-K_α radiation (λ = 0.71073 Å). The data were processed with HKL2000.[40] The structures were solved by direct methods or Patterson map interpretation for the two compounds, respectively, with SHELXS-97 and subsequent Fourier-difference synthesis and refined by full-matrix least-squares on F^2 with SHELXL-97.[41] Absorption effects were corrected empirically with the program DELABS in PLATON.[42]

In all compounds, all non-hydrogen atoms were refined with anisotropic displacement parameters. Hydrogen atoms attached to the pyridine ring were introduced at idealised positions and were treated as "riding" atoms with C(sp^2)–H = 0.93 Å and U_{iso}(H) = 1.2 times that of the parent atom. The hydrogen atoms of the water molecules (and hydroxy group when present) in the structures of $[UO_2(dipicH)_2]$·$4H_2O$, $[UO_2Rb_2(dipic)_2(H_2O)_3]$ and $[UO_2Cs_2(dipic)_2(H_2O)_4]$ were located from Fourier-difference maps and their position was refined using a constrained model (O–H = 0.86 Å or left as found; U_{iso} = 1.2 times that of the parent atom). The final Fourier-difference map for $[UO_2(dipic)(OH_2)]$ showed randomly distributed residual peaks all located in the vicinity of the U atom. No attempts were further made to locate the hydrogen atoms attached to the coordinated water molecule in this case. The molecular plots were drawn with ORTEP3[43] and SHELXTL.[41]

CCDC-279058 to -279061 contain the supplementary crystallographic data for this paper. These data can be obtained free of charge from The Cambridge Crystallographic Data Centre via www.ccdc.cam.ac.uk/data_request/cif.

Supporting Information (see footnote on the first page of this article): Solid-state luminescence spectra for $M_2UO_2(dipic)_2$, M = Li, Na, K, Rb, Cs, NBu_4; ESMS results for $[NBu_4]_2[UO_2(dipic)_2]$ in $CHCl_3$.

---

[1] P. A. Brayshaw, A. K. Hall, W. T. A. Harrison, J. M. Harrowfield, D. Pearce, T. M. Shand, B. W. Skelton, C. R. Whitaker, A. H. White, *Eur. J. Inorg. Chem.* **2005**, 1127–1141 and references cited therein.

[2] S. L. Jain, A. M. Z. Slawin, J. D. Woollins, P. Bhattacharyya, *Eur. J. Inorg. Chem.* **2005**, 721–726 and references cited therein.

[3] A. C. Gonzalez-Baró, E. E. Castellano, O. E. Piro, B. S. Parajón-Costa, *Polyhedron* **2005**, *24*, 49–55 and references cited therein.

[4] S. K. Ghosh, P. K. Bharadwaj, *Inorg. Chem.* **2004**, *43*, 2293–2298 and references cited therein.

[5] M. A. S. Goher, F. A. Mautner, A. K. Hafez, A. A. Youssef, *Polyhedron* **2003**, *22*, 515–520 and references cited therein.

[6] S. Burnet, A. K. Hall, J. M. Harrowfield, G. A. Koutsantonis, V. Sanford, D. Sauter, B. W. Skelton, A. H. White, *Supramol. Chem.* **2003**, *15*, 291–312.

[7] S. Floquet, M. Borkovec, G. Bernardinelli, A. Pinto, L.-A. Lenthold, G. Hopfgartner, D. Imbert, J.-C. G. Bünzli, C. Piguet, *Chem. Eur. J.* **2004**, *10*, 1091–1105.

[8] a) J. P. Riehl, F. S. Richardson, *Chem. Rev.* **1986**, *86*, 1–16; b) G. Muller, F. C. Muller, J. P. Riehl, *J. Alloys Compd.* **2004**, *380*, 79–83.

[9] C. Ma, C. Chen, Q. Liu, D. Liao, L. Li, *Eur. J. Inorg. Chem.* **2003**, 1227–1231.

[10] a) L. Yang, D. C. Crans, S. M. Miller, A. la Cour, O. P. Andersen, P. M. Koszynski, M. E. Godzala III, L. D. Austin, G. R. Willsky, *Inorg. Chem.* **2002**, *41*, 4859–4871; b) D. C. Crans, M. Mahroof-Tahir, M. D. Johnson, P. C. Wilkins, L. Yang, K. Robbins, A. Johnson, J. A. Alfano, M. E. Godzala III, L. D. Austin, G. R. Willsky, *Inorg. Chim. Acta* **2003**, *356*, 365–378.

[11] G. Marangoni, S. Degetto, R. Graziani, G. Bombieri, E. Forsellini, *J. Inorg. Nucl. Chem.* **1974**, *6*, 1787–1794.

[12] A. Cousson, J. Proust, E. N. Rizkalla, *Acta Crystallogr. Sect. C: Cryst. Struct. Commun.* **1991**, *47*, 2065–2069.

[13] A. Cousson, F. Nectoux, M. Pagès, E. N. Rizkalla, *Radiochim. Acta* **1993**, *61*, 177–180.

[14] Monothiocarboxylate derivative: M. P. Neu, M. T. Johnson, J. H. Matonic, B. L. Scott, *Acta Crystallogr. Sect. C: Cryst. Struct. Commun.* **2001**, *57*, 240–242.

[15] A. Immirzi, G. Bombieri, S. Degetto, G. Marangoni, *Acta Crystallogr., Sect. B: Struct. Sci* **1975**, *31*, 1023–1028.

[16] B. Masci, P. Thuéry, *Polyhedron* **2005**, *24*, 229–237.

[17] I. Wharf, T. Gramstad, M. Onyszchuk, *Can. J. Chem.* **1976**, *54*, 3430–3438.

[18] See, for example: G. A. Bowmaker, I. Bytheway, L. M. Engelhardt, J. M. Harrowfield, D. L. Kepert, H. Miyamae, J. M. Patrick, T. M. Shand, B. W. Skelton, A. A. Soudi, A. H. White, *Aust. J. Chem.* **1996**, *49*, 1026–1169.

[19] M. M. Bishop, A. H. W. Lee, L. F. Lindoy, P. Turner, B. W. Skelton, A. H. White, *J. Inclusion Phenom. Macrocyclic Chem.* **2005**, *17*, 37–45.

[20] C. Janiak, *Dalton Trans.* **2000**, 3885–3896.

[21] J. M. Harrowfield, G. S. Shahverdizadeh, A. A. Soudi, *Supramol. Chem.* **2003**, *15*, 367–373.

[22] J. M. Harrowfield, B. W. Skelton, A. H. White, *C. R. Chim.* **2005**, *8*, 169–180.

[23] a) H. D. Burrows, M. da G. Miguel, *Adv. Colloid Interface Sci.* **2001**, *89–90*, 495–496; b) S. J. Formosinho, H. D. Burrows, M. da G. Miguel, M. E. D. G. Azenha, I. M. Saraiva, A. C. D. N. Ribeiro, I. G. Khudyakov, R. G. Gasanov, M. Sarakha, *Photochem. Photobiol. Sci.* **2003**, *2*, 569–575.

[24] S. M. Fonseca, H. D. Burrows, M. da G. Miguel, M. Sarakha, M. Bolte, *Photochem. Photobiol. Sci.* **2004**, *3*, 317–321.

[25] B. Masci, personal communication.

[26] Z.-T. Yu, Z.-L. Liao, Y.-S. Jiang, G.-H. Li, J.-S. Chen, *Chem. Eur. J.* **2005**, *11*, 2642–2650.

[27] a) J. M. Harrowfield, B. W. Skelton, A. H. White, *Aust. J. Chem.* **1995**, *48*, 1311–1331; b) J. M. Harrowfield, R. P. Sharma, B. W. Skelton, A. H. White, *Aust. J. Chem.* **1998**, *51*, 707–722; J. M. Harrowfield, R. P. Sharma, B. W. Skelton, A. H. White, *Aust. J. Chem.* **1998**, *51*, 723–734; J. M. Harrowfield, R. P. Sharma, B. W. Skelton, A. H. White, *Aust. J. Chem.* **1998**, *51*, 735–746.

[28] L. Shimoni-Livny, J. P. Glusker, C. W. Bock, *Inorg. Chem.* **1998**, *37*, 1853–1867.

[29] Z. Asfari, J. M. Harrowfield, P. Thuéry, J. Vicens, *Supramol. Chem.* **2003**, *15*, 69–77.

[30] R. D. Hancock, J. H. Reibenspies, H. Maumela, *Inorg. Chem.* **2004**, *43*, 2981–2987.

[31] A. A. Soudi, F. Marandi, A. Ramazani, E. Ahmadi, A. Morsali, *C. R. Chim.* **2005**, *8*, 157–168.

[32] Y.-Z. Zheng, M.-L. Tong, X.-M. Chen, *Eur. J. Inorg. Chem.* **2005**, 4109–4117.

[33] *CrysAlis RED* (Version 1.171.24 beta), Oxford Diffraction Ltd., Oxford, United Kingdom, **2005**.

[34] L. J. Farrugia, *J. Appl. Crystallogr.* **1999**, *32*, 837–838.

[35] A. Altomare, G. Cascarano, C. Giacovazzo, A. Guagliardi, *J. Appl. Crystallogr.* **1993**, *26*, 343–350.

[36] SHELX97 [Includes SHELXS97, SHELXL97, CIFTAB]; *Programs for Crystal Structure Analysis* (Release 97–2). G. M. Sheldrick, Institute for inorganic chemistry, University of Göttingen, Göttingen, Germany, **1998**.

[37] N. W. Alcock, **1970**, *The Analytical Method for Absorption Correction* (Eds.: F. R Ahmed, S. R. Hall, C. P. Huber), Crystallographic Computing, Munksgaard, Copenhagen, pp. 271–278.

[38] R. H. Blessing, *Acta Crystallogr., Sect. A: Found. Crystallogr.* **1995**, *51*, 33–38.

[39] *Kappa-CCD Software*, Nonius BV, Delft, The Netherlands, **1998**.

[40] Z. Otwinowski, W. Minor, *Methods Enzymol.* **1997**, *276*, 307–326.

[41] G. M. Sheldrick, SHELXTL, Version 5.1, Bruker AXS Inc., Madison, WI, USA, **1999**.

[42] A. L. Spek, PLATON, University of Utrecht, The Netherlands, **2000**.

[43] L. J. Farrugia, *J. Appl. Crystallogr.* **1997**, *30*, 565.

Received: July 27, 2005